Journal of Engineering Physics and Thermophysics, Vol. 83, No. 3, 2010

ON LOCALIZATION OF CONTACT SURFACES IN MULTIFLUID HYDRODYNAMICS

V. S. Surov

UDC 532.529.5

Within the framework of the unified-equilibrium model of a multicomponent mixture that accounts for the forces of interfractional interaction, the problem of localization of contact surfaces is solved numerically in Euler variables. A finite-volume conservative scheme with the approximate Riemann solver HLLC was used in the calculations.

Keywords: *single-velocity multicomponent medium, contact boundaries, approximate Riemann solver HLLC, numerical simulation.*

Introduction. There are several approaches described in the literature, with the use of which in Euler variables the problem of determining the positions of contact boundaries between different ideal compressible fluids is solved. In some of these, interfaces are modeled by weightless markers moving in space [1], in others the methods of VOF [2], level set [3], concentrations [4, 5], etc. are used to fix contact boundaries.

We will consider briefly the techniques of localization of contact boundaries available in the literature. To simplify the representation, we will restrict the consideration to a one-dimensional approximation.

In the Y model [6] the following equations that describe the joint motion of two media are given:

$$\frac{\partial \rho}{\partial t}+\frac{\partial \rho u}{\partial x}=0\,,\quad \frac{\partial \rho u}{\partial t}+\frac{\partial\left(\rho u^2+p\right)}{\partial x}=0\,,\quad \frac{\partial \rho e}{\partial t}+\frac{\partial(\rho e+p)\,u}{\partial x}=0\,; \tag{1}$$

$$\frac{\partial Y_1}{\partial t}+u\,\frac{\partial Y_1}{\partial x}=0\,, \tag{2}$$

where $e=\varepsilon+\frac{1}{2}u^2$ is the specific total energy of the mixture; Y_i is the mass portion of the ith fraction (i = 1, 2). System (1)–(2) is considered together with the equation of state of the mixture:

$$\varepsilon=\frac{p}{\rho\,(\gamma-1)}\,, \tag{3}$$

which coincides with the equation of state of an ideal gas. To calculate γ, the following expression is used:

$$\gamma=\frac{c_{v1}\gamma_1 Y_1+c_{v2}\gamma_2 Y_2}{c_{v1}Y_1+c_{v2}Y_2}\,, \tag{4}$$

where c_{vi} is the heat capacity of the ith gas at a constant volume; γ_i is the adiabatic index, and $Y_2 = 1 - Y_1$. In the limiting cases, where $Y_1 = 1$ or $Y_1 = 0$, expressions (1)–(4) are reduced to the corresponding relations for "pure" gases with the adiabatic indices γ_1 and γ_2. It can be easily verified that the system of equations (1)–(2) relates to the hyperbolic type. The roots of the characteristic equation are the real numbers $\lambda_1 = u - c$, $\lambda_2 = \lambda_3 = u$, and $\lambda_4 = u + c$, where

South Urals State University, 76 Lenin Ave., Chelyabinsk, 454080. Russia; email: svs@csu.ru. Translated from Inzhenerno-Fizicheskii Zhurnal, Vol. 83, No. 3, pp. 518–527, May–June, 2010. Original article submitted May 16, 2009.

1062-0125/10/8303-0549©2010 Springer Science+Business Media, Inc.

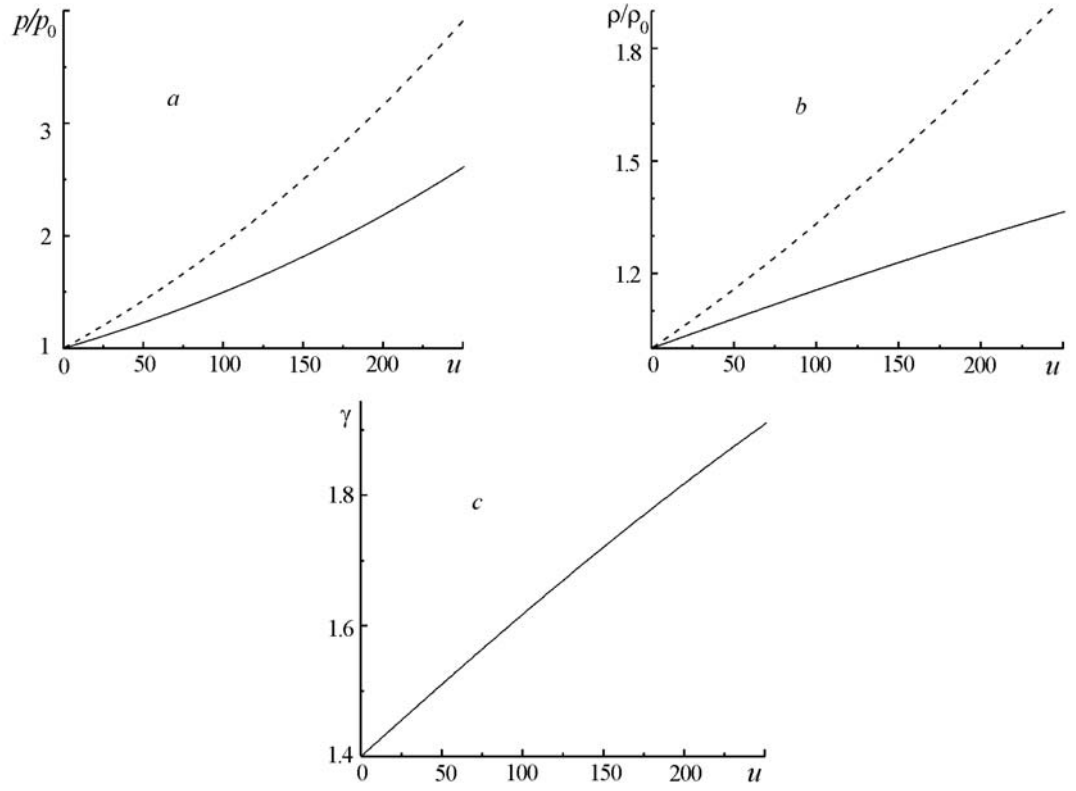

Fig. 1. Dependences of p/p_0 (a), ρ/ρ_0 (b), and γ (c) on u according to the γ model (solid curves) and the ideal gas model (dashed) curves.

$$c = \sqrt{\frac{p}{\rho}\left(\frac{c_{v1}\gamma_1 Y_1 + c_{v2}\gamma_2 Y_2}{c_{v1}Y_1 + c_{v2}Y_2}\right)} \,. \tag{5}$$

The sphere of application of the Y model is limited to mixtures of ideal gases.

In the γ model (see [6]) it is possible to calculate the joint motion of not only ideal gases, but also of media described with the use of more complex equations of state. In [7] the γ model was used for media with the Van der Waals equations of state and in [8] with the Mie–Grüneisen equations of state, etc. For ideal gases Eq. (2) is replaced by the so-called "topological" equation:

$$\frac{\partial \gamma}{\partial t} + u\frac{\partial \gamma}{\partial x} = 0 \,, \tag{6}$$

i.e., it is assumed that the adiabatic index γ is a variable quantity ($\gamma_1 \le \gamma \le \gamma_2$, if $\gamma_1 < \gamma_2$; $\gamma_2 \le \gamma \le \gamma_1$ in the opposite case). System (1) and (6) is hyperbolic with the roots of the characteristic equation $\lambda_1 = u - c$, $\lambda_2 = \lambda_3 = u$, and $\lambda_4 = u + c$, where

$$c = \sqrt{\frac{\gamma p}{\rho}} \,. \tag{7}$$

In a number of cases the γ model yields acceptable results; however, for gases with greatly differing densities, substantial errors in calculations of the parameters in the vicinity of contact boundaries are possible. As an example, we will consider the limiting case, viz., we will calculate the reflection of a shock wave propagating from a rigid wall through a stationary gas ($\gamma = 1.4$, $\rho_0 = 1.24$ kg/m^3, $p_0 = 10^5$ Pa).

Figure 1 presents the dependences of the dimensionless pressure, density, as well as of γ on u in the shock wave reflected from a barrier. The dependences were calculated by the γ model and the model of an ideal gas, and they show that with increase in the velocity behind the incident wave front the error in the determination of the parameters behind the reflected shock wave increases when the γ model is used. To exclude such kinds of results, it was suggested in [6] to replace Eq. (6) by the expression

$$\frac{\partial \psi}{\partial t} + u \frac{\partial \psi}{\partial x} = 0 , \tag{8}$$

where

$$\gamma(\psi) = \begin{cases} \gamma_1 , & \text{if} \quad \psi > 0 , \\ \gamma_2 , & \text{if} \quad \psi < 0 . \end{cases} \tag{9}$$

The use of these equations excludes the possibility of a change in γ in reflected shock waves. In [9], more complex modifications of Eqs. (8) and (9) were suggested.

In the α model [10], the key role is played by the volume concentration of one of the fractions. The equations of the model include the laws of mass, momentum, and energy concentration for a mixture as a whole (1), as well as

$$\frac{\partial \alpha_1 \rho_1^0}{\partial t} + u \frac{\partial \alpha_1 \rho_1^0}{\partial x} = 0 , \tag{10}$$

$$\frac{\partial \alpha_1}{\partial t} + u \frac{\partial \alpha_1}{\partial x} = 0 , \tag{11}$$

where α_i and ρ_i^0 are the volume concentration and the true density of the ith fraction of the mixture (i = 1, 2). Relation (10) represents the mass conservation law for the 1st fraction of the mixture, whereas Eq. (11) is an analog of the topological equation (6) of the previous model. It should be noted that Eq. (11) has no strict physical justification. Bearing in mind the equality $\varepsilon = \varepsilon(p, \rho, \rho_1^0, \alpha_1)$, we can show that the system of equations (1), (10)–(11) is hyperbolic with the roots of the characteristic equation:

$$\lambda_1 = u - c , \quad \lambda_2 = \lambda_3 = \lambda_4 = u , \quad \lambda_5 = u + c ,$$

where

$$c = \sqrt{\left(\frac{\partial \varepsilon}{\partial p}\right)^{-1} \left(\frac{p}{\rho^2} - \frac{\rho_1^0}{\rho} \frac{\partial \varepsilon}{\partial \rho_1^0} - \frac{\partial \varepsilon}{\partial \rho}\right)} . \tag{12}$$

If, in describing the behavior of the mixture components, we use the equation of state of the form

$$\varepsilon_i = \frac{p - c_{*i}^2 (\rho_i^0 - \rho_{*i})}{\rho_i^0 (\gamma_i - 1)} , \tag{13}$$

where γ_i, ρ_{*i}, c_{*i} are constants of the ith fraction which account for its individual properties, then the expression for the specific internal energy of the mixture will take the form

$$\varepsilon = \frac{1}{p} \left[b_2 + p B_2 + \alpha_1 (p B_{12} - d_{12} \rho_1^0 + b_{12}) \right] - d_2 , \tag{14}$$

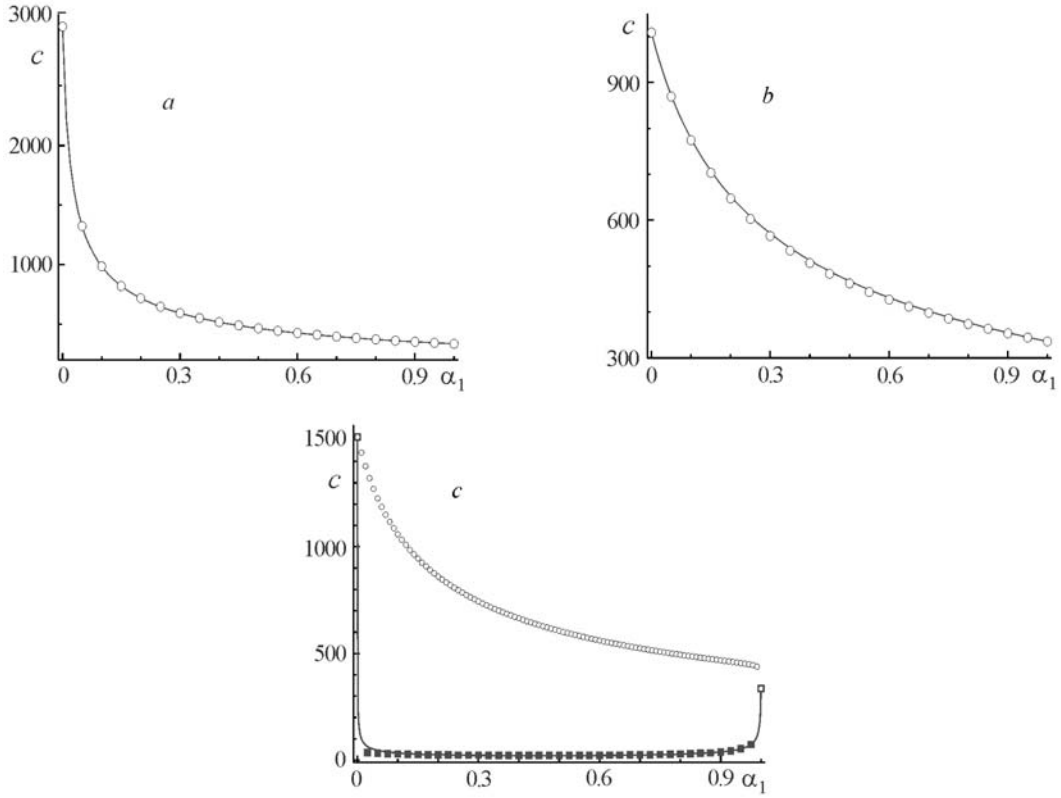

Fig. 2. Dependences of the speed of sound on α_1 in the mixture: a) air–hydrogen; b) air–helium; c) air-water. Calculations by the α model, open circles; by the modified α model, black squares; by the UE model, solid curves.

where

$$B_1 = 1/(\gamma_1 - 1)\,; \quad B_2 = 1/(\gamma_2 - 1)\,; \quad B_{12} = B_1 - B_2\,; \quad d_1 = c_{*1}^2 B_1\,; \quad d_2 = c_{*2}^2 B_2\,; \quad d_{12} = d_1 - d_2\,;$$

$$b_1 = d_1 \rho_{*1}\,; \quad b_2 = d_2 \rho_{*2}\,; \quad b_{12} = b_1 - b_2\,.$$

Figure 2 presents the graphs of the dependences of the speeds of sound on α_1 in the air–hydrogen, air–helium, and air–water mixtures; the graphs were calculated by the α model and the unified equilibrium (UE) model (see below). It is seen from this figure that for a mixture of gases the speeds of sound in both models are close. However, if we consider the water–air mixture, the results of the computation of the speeds of sound differ substantially. It should be noted that the values of the speed of sound calculated within the frame of the UE model agree well with experiment.

Due to the difference between the calculated values for the speed of sound in gas-liquid mixtures with experiment, the α model was modified in [11]. Instead of Eq. (11) the following relation was suggested:

$$\frac{\partial \alpha_1}{\partial t} + u \frac{\partial \alpha_1}{\partial x} = A \frac{\partial u}{\partial x}\,, \tag{15}$$

where

$$A = \frac{\rho_2^0 c_2^2 - \rho_1^0 c_1^2}{\dfrac{\rho_1^0 c_1^2}{\alpha_1} + \dfrac{\rho_2^0 c_2^2}{\alpha_2}}\,. \tag{16}$$

For the two-term equation of state (13) used in describing the properties of fluids, the speeds of sound in Eq. (16) are determined as

$$c = \sqrt{\frac{\gamma_i (p + p_{*i})}{\rho_i^0}}. \tag{17}$$

Here $p_{*i} = \rho_{*i} c_{*i}^2 / \gamma_i$. The system of equations (1), (8), and (15) is also related to a hyperbolic type with the roots of the characteristic equation $\lambda_1 = u - c$, $\lambda_2 = \lambda_3 = \lambda_4$, and $\lambda_5 = u + c$, where

$$c = \sqrt{\left(\frac{\partial \varepsilon}{\partial p}\right)^{-1} \left[\frac{p}{\rho^2} + \frac{A}{\rho} \frac{\partial \varepsilon}{\partial \alpha_i} - \frac{\rho_1^0}{\rho} \left(\frac{A}{\alpha_1} + 1\right) \frac{\partial \varepsilon}{\partial \rho_i^0} - \frac{\partial \varepsilon}{\partial \rho}\right]}. \tag{18}$$

For a particular case of the equations of state in the form of Eq. (13), Eq. (18) will be rewritten as

$$c = \sqrt{\frac{b_2 + p\,(1 + B_2) + (A + \alpha_1)\,(b_{12} + pB_{12})}{\rho\,(B_2 + \alpha_1 B_{12})}}. \tag{19}$$

In Fig. 2c the dependence of the speed of sound on α_1 calculated with the use of Eq. (19) is denoted by open circles; it appears to be close to that obtained by the UE model (the solid curve).

Calculation of the Motion of Contact Boundaries within the Framework of the UE Model. Many difficulties connected with the use of the above-described approaches can be avoided by using the UE model, which accounts for the forces of interfractional interaction (see [12]). The UE model does not involve any "nonphysical" equations of the form of Eq. (6) or (11). For the UE model the problem is formulated as follows. It is required to calculate the simultaneous flow of n different ideal compressible fluids separated from one another by contact boundaries. The motions of each of the media that occupy some finite (not obligatorily connected) volumes V_j (j = 1, ..., n) are described by the Euler equations. To solve the problem posed it is necessary that at the initial time (t = 0) the volume concentrations of the fractions in a mixture satisfy the equalities $\alpha_{ij} = \delta_{ij}$ ($\forall x \in V_j$), where δ_{ij} is the Kronecker delta function.

The equations that describe the joint motion of the media are as follows (see [12]):

$$\frac{\partial \rho}{\partial t} + (\mathbf{u}\cdot\nabla)\,\rho + \rho \operatorname{div} \mathbf{u} = 0\,, \quad \frac{\partial \mathbf{u}}{\partial t} + (\mathbf{u}\cdot\nabla)\,\mathbf{u} + \frac{1}{\rho} \operatorname{grad} p = 0\,, \quad \frac{\partial p}{\partial t} + (\mathbf{u}\cdot\nabla)\,p + \rho c^2 \operatorname{div} \mathbf{u} = 0\,;$$

$$\frac{\partial \rho_i^0}{\partial t} + (\mathbf{u}\cdot\nabla)\,\rho_i^0 + \rho_i^0 G_i \operatorname{div} \mathbf{u} = 0\,, \tag{20}$$

$$\frac{\partial \alpha_i}{\partial t} + (\mathbf{u}\cdot\nabla)\,\alpha_i + \alpha_i (1 - G_i) \operatorname{div} \mathbf{u} = 0\,, \quad i = 1, ..., n - 1\,,$$

where

$$G_i = \frac{1}{\rho_i^0} \left(\frac{\partial \varepsilon_i}{\partial \rho_i^0}\right)^{-1} \left(\frac{p}{\rho_i^0} - \rho c^2 \frac{\partial \varepsilon_i}{\partial p}\right).$$

Here

$$c = \sqrt{\frac{\frac{p}{\rho} - \rho\frac{\partial\varepsilon}{\partial\rho} - \sum_{i=1}^{n-1}\left[\frac{p}{\rho_i^0}\frac{\partial\varepsilon}{\partial\rho_i^0}\left(\frac{\partial\varepsilon_i}{\partial\rho_i^0}\right)^{-1} + \alpha_i\frac{\partial\varepsilon}{\partial\alpha_i}\left(1 - p\left((\rho_i^0)^2\frac{\partial\varepsilon_i}{\partial\rho_i^0}\right)^{-1}\right)\right]}{\rho\left[\frac{\partial\varepsilon}{\partial p} + \sum_{i=1}^{n-1}\frac{\partial\varepsilon_i}{\partial p}\left(\frac{\partial\varepsilon_i}{\partial\rho_i^0}\right)^{-1}\left(\frac{\alpha_i}{\rho_i^0}\frac{\partial\varepsilon}{\partial\alpha_i} - \frac{\partial\varepsilon}{\partial\rho_i^0}\right)\right]}} \,. \tag{21}$$

It is assumed that in describing the thermodynamic properties of each of the fractions the caloric equations of state are used, which in the general case have the form $\varepsilon_i = \varepsilon_i(p, \rho_i^0)$. The relation for the specific internal energy of the mixture ε is defined by the equality

$$\varepsilon(\rho, p, \alpha_1, \rho_1^0, ..., \alpha_{n-1}, \rho_{n-1}^0) = \frac{1}{\rho}\sum_{i=1}^{n-1}\alpha_i\rho_i^0\varepsilon_i \,. \tag{22}$$

For one-dimensional flows system (20) will be rewritten in vector-matrix form as

$$\frac{\partial\mathbf{U}}{\partial t} + \mathrm{A}\frac{\partial\mathbf{U}}{\partial x} = 0 \,, \tag{23}$$

where

$$\mathbf{U} = (\rho, u, p, \rho_1^0, \alpha_1, ..., \rho_{n-1}^0, \alpha_{n-1})^T \,,$$

$$\mathbf{A} = \begin{pmatrix}
u & \rho & 0 & 0 & 0 & \dots & 0 & 0 & 0 & \dots & 0 \\
0 & u & 1/\rho & 0 & 0 & \dots & 0 & 0 & 0 & \dots & 0 \\
0 & \rho c^2 & u & 0 & 0 & \dots & 0 & 0 & 0 & \dots & 0 \\
0 & \rho_i^0 G_1 & 0 & u & 0 & \dots & 0 & 0 & 0 & \dots & 0 \\
0 & \alpha_1(1-G_1) & 0 & 0 & u & \dots & 0 & 0 & 0 & \dots & 0 \\
\dots & \dots & \dots & \dots & \dots & \dots & \dots & \dots & \dots & \dots & \dots \\
0 & \rho_{n-1}^0 G_{n-1} & 0 & 0 & 0 & \dots & u & 0 & 0 & \dots & 0 \\
0 & \alpha_{n-1}(1-G_{n-1}) & 0 & 0 & 0 & \dots & 0 & u & 0 & \dots & 0
\end{pmatrix}.$$

As shown in [12], the system of equations (20) is hyperbolic with the roots of the characteristic equation $\lambda_1 = u - c$, $\lambda_2 = ... = \lambda_{2n} = \lambda_c = u$, and $\lambda_{2n+1} = u + c$.

If in describing the behavior of the mixture components we use the equation of state of the form of (13), then the expression for the specific internal energy of the mixture (22) takes the form

$$\varepsilon = \frac{1}{\rho}\left[\sum_{i=1}^{n-1}\alpha_i(pB_{in} - d_{in}\rho_i^0 + b_{in} + pB_n + b_n\right] - d_n \,, \tag{24}$$

and the relation for the speed of sound, Eq. (21), is rewritten as

$$c = \sqrt{\frac{b_n + p\left[1 + B_n - \sum_{i=1}^{n-1}\frac{\alpha_i(b_{in} + pB_{in})}{b_i + pB_i}\right]}{\rho\left[B_n + \sum_{i=1}^{n-1}\frac{\alpha_i(b_nB_i - b_iB_n)}{b_i + pB_i}\right]}} \,, \tag{25}$$

where

$$B_i = 1/(\gamma_i - 1)\,;\quad B_{in} = B_i - B_n\,;\quad d_i = c_{*i}^2 B_i\,;\quad d_{in} = d_i - d_n\,;\quad b_i = d_i \rho_{*i}\,;\quad b_{in} = b_i - b_n\,.$$

We will consider a one-dimensional plane flow of a binary mixture consisting of an ideal gas with adiabatic index γ and the second compressible component whose parameters are described with the use of the two-term equation of state (13).

In calculation of mixture flows the following procedure was used. Since the first component of the mixture is an ideal gas for which $b_1 = 0$, the equation of heat influx for this fraction, considered together with the continuity equation for the mixture as a whole, is reduced to a divergent form:

$$\frac{\partial \rho\varphi_1}{\partial t} + \frac{\partial \rho\varphi_1 u}{\partial x} = 0\,,$$

where $\varphi_1 = \ln\left[\frac{1}{\rho_1}\left(\frac{p}{\rho_1^0}\right)^{B_1}\right]$. Thus, if we introduce the vector $\mathbf{V} = (\rho,\ \rho u,\ \rho e,\ \rho_1,\ \rho\varphi_1)^T$, then the governing system of equations (23) with the parameters

$$\mathbf{U} = \begin{pmatrix} \rho \\ u \\ p \\ \rho_1^0 \\ \alpha_1 \end{pmatrix},\quad \mathrm{A} = \begin{pmatrix} u & \rho & 0 & 0 & 0 \\ 0 & u & 1/\rho & 0 & 0 \\ 0 & \rho c^2 & u & 0 & 0 \\ 0 & \rho_1^0 G_1 & 0 & u & 0 \\ 0 & \alpha_1 (1 - G_1) & 0 & 0 & u \end{pmatrix}$$

subject to the equation of state (24), will take the form

$$\frac{\partial \mathbf{V}}{\partial t} + \frac{\partial \Pi(\mathbf{V})}{\partial x} = 0\,, \tag{26}$$

where $\mathbf{V} = (\rho,\ \rho u,\ \rho e,\ \rho_1,\ \rho\varphi_1)^T$, $\Pi(\mathbf{V}) = (\rho u,\ p + \rho u^2,\ (p + \rho e)u,\ \rho_1 u,\ \rho\varphi_1 u)^T$. In the latter expression it is necessary to go over from the "primary" variables U_i to the new variables V_i, which can be done by making use of the equalities

$$\rho \equiv U_1 = V_1\,,\quad u \equiv U_2 = \frac{V_2}{V_1}\,,\quad p \equiv U_3 = \frac{V_4}{\alpha_1}\left[V_4 \exp\left(\frac{V_5}{V_1}\right)\right]^{\frac{1}{B_1}},$$

$$\rho_1^0 \equiv U_4 = \frac{V_4}{\alpha_1}\,,\quad \alpha_1 \equiv U_5 = -\frac{A + \sqrt{A^2 - b_{12}B}}{2b_{12}}\,,\quad e = \frac{V_3}{V_1}\,,\quad \varphi_1 = \frac{V_5}{V_1}\,,$$

$$A = b_2 - d_2 V_1 - V_3 - d_{12} V_4 + \frac{V_2^2}{2V_1} + B_{12} V_4 \left[V_4 \exp\left(\frac{V_5}{V_1}\right)\right]^{\frac{1}{B_1}},\quad B = B_2 V_4 \left[V_4 \exp\left(\frac{V_5}{V_1}\right)\right]^{\frac{1}{B_1}}.$$

The finite-volume scheme for the system in the divergent form (26) looks like

$$\frac{\mathbf{V}_i^{k+1} - \mathbf{V}_i^k}{\Delta t} + \frac{\Pi_{i+1/2}^k - \Pi_{i-1/2}^k}{\Delta x} = 0\,. \tag{27}$$

If in calculating the flows through the faces of the cells one uses the approximate solver of the Riemann problem HLL (see [13]) of the form

$$\Pi_{l-1/2}^{k}=\begin{cases}\Pi_{l-1}^{k}, & \text{if } \lambda_1>0,\\ \dfrac{\lambda_5\Pi_{l-1}^{k}-\lambda_1\Pi_{l}^{k}+\lambda_1\lambda_5\,(\mathbf{V}_{l}^{k}-\mathbf{V}_{l-1}^{k})}{\lambda_5-\lambda_1}, & \text{if } \lambda_1<0,\ \lambda_5>0 \quad (l=i,\,i+1),\\ \Pi_{l}^{k}, & \text{if } \lambda_5<0,\end{cases}$$

then loss of accuracy occurs near the contact boundary. Substantially better results are attained, if instead of the HLL one uses the approximate Riemann solver HLLC:

$$\Pi_{l-1/2}^{k}=\begin{cases}\Pi_{l-1}^{k}, & \text{if } \lambda_1\geq 0,\\ \Pi_{(l-1/2)-}^{k}, & \text{if } \lambda_1<0,\ \lambda_c\geq 0,\\ \Pi_{(l-1/2)+}^{k}, & \text{if } \lambda_c<0,\ \lambda_5\geq 0,\\ \Pi_{l}^{k}, & \text{if } \lambda_5<0,\end{cases} \tag{28}$$

that takes into account the values of the parameters on the contact boundary. Conversely, in (28) the fluxes $\Pi_{(i-1/2)-}^{k}$ and $\Pi_{(i-1/2)+}^{k}$ are defined using the following iteration procedure from [14]:

$$p_{(i-1/2)-}^{k(s+1)}-p_{i-1}^{k}+a_1\,(u_{(i-1/2)-}^{k(s+1)}-u_{i-1}^{k})=0,\quad p_{(i-1/2)-}^{k(s+1)}-p_{i}^{k}-a_2\,(\rho_{(i-1/2)-}^{k(s+1)}-\rho_{i}^{k})=0,$$

$$\alpha_{(i-1/2)-}^{k(s+1)}-\alpha_{i-1}^{k}-a_3\,(\rho_{(i-1/2)-}^{k(s+1)}-\rho_{i-1}^{k})=0,\quad \rho_{(i-1/2)-}^{0k(s+1)}=\rho_{i-1}^{0k}\,\frac{\alpha_{i-1}^{k}\rho_{(i-1/2)-}^{k(s+1)}}{\alpha_{(i-1/2)-}^{k(s+1)}\rho_{i-1}^{k}};$$

$$p_{(i-1/2)+}^{k(s+1)}-p_{i}^{k}+a_4\,(u_{(i-1/2)-}^{k(s+1)}-u_{i}^{k})=0,\quad p_{(i-1/2)+}^{k(s+1)}-p_{i}^{k}-a_5\,(\rho_{(i-1/2)+}^{k(s+1)}-\rho_{i}^{k})=0,$$

$$\alpha_{(i-1/2)+}^{k(s+1)}-\alpha_{i}^{k}-a_6\,(\rho_{(i-1/2)+}^{k(s+1)}-\rho_{i}^{k})=0,\quad \rho_{(i-1/2)+}^{0k(s+1)}=\rho_{i}^{0k}\,\frac{\alpha_{i}^{k}\rho_{(i-1/2)+}^{k(s+1)}}{\alpha_{(i-1/2)+}^{k(s+1)}\rho_{i}^{k}}, \tag{29}$$

$$p_{(i-1/2)-}^{k(s+1)}=p_{(i-1/2)+}^{k(s+1)},\quad u_{(i-1/2)-}^{k(s+1)}=u_{(i-1/2)+}^{k(s+1)},$$

where

$$a_1=\frac{1}{2}\,((\rho c)_{i-1}^{k}+(\rho c)_{(i-1/2)-}^{k(s)});\quad a_2=\frac{1}{2}\,((c^2)_{i-1}^{k}+(c^2)_{(i-1/2)-}^{k(s)});$$

$$a_3=\frac{1}{2}\left(\frac{\alpha_{i-1}^{k}\,(1-G_{i-1}^{k})}{\rho_{i-1}^{k}}+\frac{\alpha_{(i-1/2)-}^{k(s)}\,(1-G_{(i-1/2)-}^{k(s)})}{\rho_{(i-1/2)-}^{k(s)}}\right);$$

$$a_4=\frac{1}{2}\,((\rho c)_{i}^{k}+(\rho c)_{(i-1/2)+}^{k(s)});\quad a_5=\frac{1}{2}\,((c^2)_{i}^{k}+(c^2)_{(i-1/2)+}^{k(s)});$$

$$a_6=\frac{1}{2}\left(\frac{\alpha_{i}^{k}\,(1-G_{i}^{k})}{\rho_{i}^{k}}+\frac{\alpha_{(i-1/2)+}^{k(s)}\,(1-G_{(i-1/2)+}^{k(s)})}{\rho_{(i-1/2)+}^{k(s)}}\right).$$

The subscripts "+" and "−" stand for values of the parameters on the contact boundaries between the cells $i-1$ and i as well as between i and $i+1$ are from their left and right sides, respectively (see Fig. 3). Expressions (29) are the finite-difference representations of the characteristic relations of the UE model.

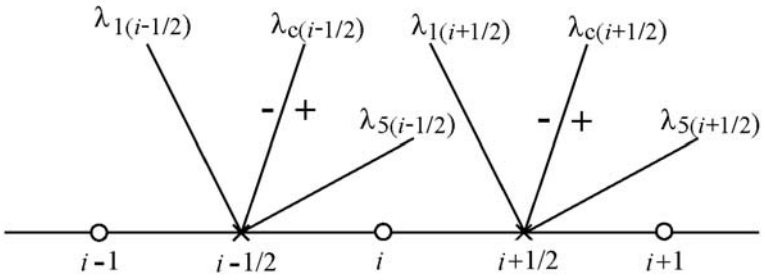

Fig. 3. Schematic diagram of the method of calculation.

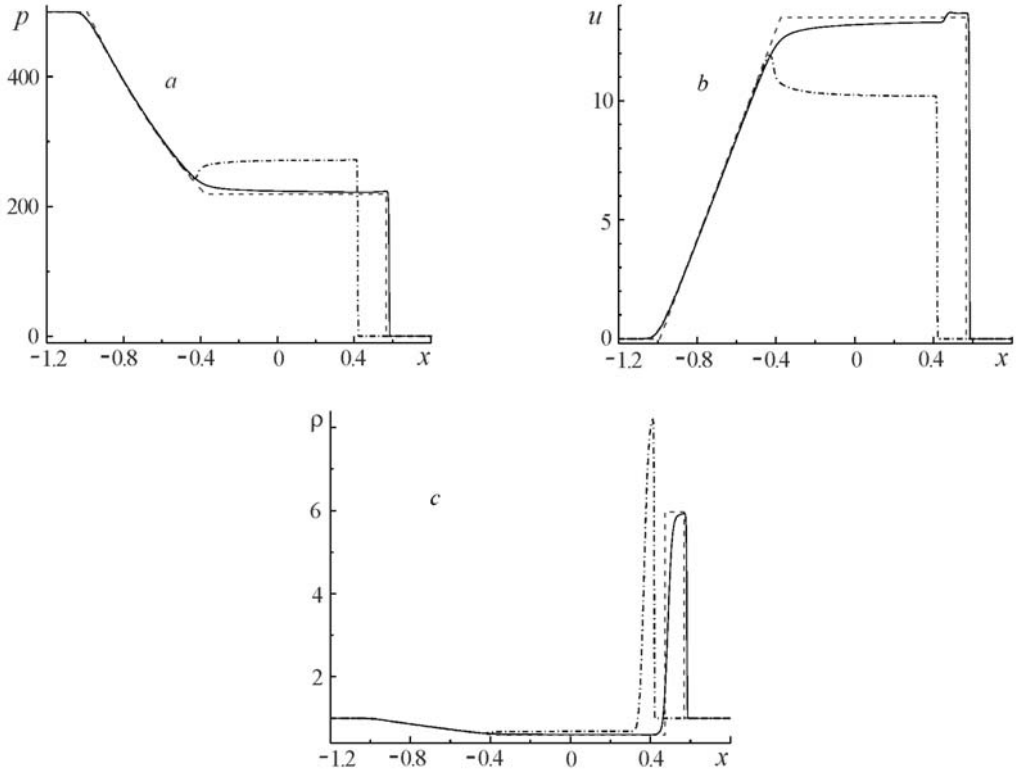

Fig. 4. Functions $p(x)$ (a), $u(x)$ (b), and $\rho(x)$ (c) by the time instant $t = 0.035$: numerical calculation, solid curves; exact solution, dashed curves; solution by the CIR method, dashed-dotted curves.

The possibilities of the above-described numerical method applied for the localization of contact boundaries will be considered using as an example the Riemann problem at the following values of the parameters at time $t = 0$: "on the left" ($x < 0$) from the contact boundary that separates different gases, $-(p, u, \rho, \gamma)_L = (500, 0, 1, 1.6)$; "on the right" from it ($x > 0$) $(p, u, \rho, \gamma)_L = (0.2, 0, 1, 1.4)$.

Figure 4 presents the data of numerical calculations for flows that were obtained by the time instant $t = 0.035$ (solid curves). The dashed curve represents the exact solution of the Riemann problem. The available discrepancy between the numerical and exact solutions is attributable to the absence of any correction of the parameters in the vicinity of the contact boundary. The calculations were carried out using Eqs. (27)–(29) in a "through" manner in contrast to the procedures of the type of level set and Ghost in which the position of the contact boundary was reconstructed in different ways. It should also be noted that the application of the "classical" finite-difference schemes in solving the problems of the dynamics of multifluid media leads either to extremely distorted results or even to an emergency halt of the program because of the strong pulsations of the values of the parameters near the contact boundary (when using, for example, schemes of the McCormack or Lax–Wendroff types). As an example, Fig. 4 presents the distribu-

tions of the pressure $p(x)$, velocity $u(x)$, and of the density $\rho(x)$ obtained with the use of one of the modified Courant–Isaacson–Rees schemes (CIR, see [13]):

$$\frac{\mathbf{U}_i^{k+1} - \mathbf{U}_i^k}{\Delta t} + (\Omega^{-1}\Lambda^{-}\Omega)_{i+1/2}^k \frac{\mathbf{U}_{i+1}^k - \mathbf{U}_i^k}{\Delta x} + (\Omega^{-1}\Lambda^{+}\Omega)_{i-1/2}^k \frac{\mathbf{U}_i^k - \mathbf{U}_{i-1}^k}{\Delta x} = 0\,, \tag{30}$$

where $\Lambda^{\pm} = \frac{1}{2}(\Lambda \pm |\Lambda|)$. Computations were made on the same finite-difference grid and were obtained by the same moment by which the previous calculations were made. The matrices Ω, Λ, and Ω^{-1} from (30) have the form

$$\Omega = \begin{pmatrix} 0 & -\rho c & 1 & 0 & 0 \\ -c^2 & 0 & 1 & 1/h_1 & -1/g_1 \\ -c^2 & 0 & 1 & 0 & 0 \\ -1/\rho & 0 & 0 & 1/h_1 & 0 \\ 0 & \rho c & 1 & 0 & 0 \end{pmatrix}, \quad \Lambda = \begin{pmatrix} u-c & 0 & 0 & 0 & 0 \\ 0 & u & 0 & 0 & 0 \\ 0 & 0 & u & 0 & 0 \\ 0 & 0 & 0 & u & 0 \\ 0 & 0 & 0 & 0 & u+c \end{pmatrix},$$

$$\Omega^{-1} = \begin{pmatrix} \frac{1}{2c^2} & 0 & -\frac{1}{c^2} & 0 & \frac{1}{2c^2} \\ -\frac{1}{2\rho c} & 0 & 0 & 0 & \frac{1}{2\rho c} \\ \frac{1}{2} & 0 & 0 & 0 & \frac{1}{2} \\ \frac{h_1}{2\rho c^2} & 0 & -\frac{h_1}{\rho c^2} & h_1 & \frac{h_1}{2\rho c^2} \\ \frac{g_1}{2\rho c^2} & -g_1 & \frac{(\rho c^2 - 1)g_1}{\rho c^2} & g_1 & \frac{g_1}{2\rho c^2} \end{pmatrix},$$

where $h_1 = \rho_1^0 G_1$; $g_1 = \alpha_1(1 - G_1)$.

Conclusions. Within the framework of the unified-equilibrium model of a multicomponent mixture the problem on the motion of multifluid media has been solved in Euler variables. The approximate Riemann solver HLLC was described, which takes into account the values of the parameters on the contact boundary, the application of which in the finite-volume scheme makes it possible to obtain nonoscillating solutions satisfactorily coinciding with the available exact values.

NOTATION

c, adiabatic speed of sound in a mixture; c_{*i}, a constant in the equation of state; $\mathbf{F}$, mass force density; J_{ij}, intensity of the conversion of mass from the ith fraction into the jth one in a unit volume of the mixture; p, pressure; Q_{ij}, heat release per unit time per unit volume of the mixture occurring as a result of the conversion of ith fraction into the jth one; R_{ij}, quantity of heat per unit time per unit volume of the mixture entering into the ith fraction from the jth one by radiation; t, time; $\mathbf{u}(u)$, vector (component) of velocity; x, spatial variable; α_i, volume concentration of ith fraction; γ_i, a constant of the equation of state; ε_i, specific internal energy; ρ, density of the mixture; ρ_i^0, true density of the ith fraction; $\rho_i = \alpha_i\rho_i^0$, reduced density of the ith fraction; ρ_{*i}, a constant of the equation of state. Subscripts and superscripts: 0, in a nonperturbed medium; c, L, and R, for the parameters at the contact discontinuity "on the left" and "on the right" from it; k, time layer; (s), iteration number; T, transposition operator.

REFERENCES

1. J. Glimm, J. Grove, X. Li, and D. Tan, Robust computational algorithms for dynamic interface tracking in three dimensions, *SIAM J. Sci. Comput.*, **21**, No. 6, 2240–2276 (2000).

2. R. Scardovelli and S. Zaleski, Direct numerical simulation of free-surface and interfacial flow, *Annu. Rev. Fluid Mech.*, **31**, 567–598 (1999).
3. S. Osher and R. P. Fedkiw, A level set method: An overview and some recent results, *J. Comput. Phys.*, **169**, 463–502 (2001).
4. S. M. Bakhrakh, Yu. P. Glagoleva, M. S. Samigulin, et al., Calculation of gasdynamic flows based on the method of concentrations, *Dokl. Akad. Nauk SSSR*, **257**, No. 3, 566–569 (1981).
5. Yu. A. Bondarenko and Yu. V. Yanilkin, Calculation of the thermodynamic parameters of mixed cells in gas dynamics, *Mat. Modelir.*, **15**, No. 6, 63–81 (2002).
6. R. Abgrall and S. Karni, Computations of compressible multifluids, *J. Comput. Phys.*, **169**, 594–623 (2001).
7. Keh-Ming Shyue, A fluid-mixture type algorithm for compressible multicomponent flow with Van der Waals equation of state, *J. Comput. Phys.*, **156**, 43–88 (1999).
8. Keh-Ming Shyue, A fluid-mixture type algorithm for compressible multicomponent flow with Mie–Gruneisen equation of state, *J. Comput. Phys.*, **171**, 678–707 (2001).
9. I. É. Ivanov and I. A. Kryukov, Numerical simulation of flows of a multicomponent gas with strong discontinuities of the mixture properties, *Mat. Modelir.*, **19**, No. 12, 89–100 (2007).
10. G. Allaire, S. Clerc, and S. Kokh, A five-equation model for the simulation of interfaces between compressible fluids, *J. Comput. Phys.*, **181**, 577–616 (2002).
11. A. Murrone and H. Guillard, A five-equation reduced model for compressible two-phase flow problems, *J. Comput. Phys.*, **202**, 664–698 (2005).
12. V. S. Surov, Single-velocity model of a heterogeneous medium with a hyperbolic adiabatic core, *Zh. Vych. Mat. Mat. Fiz.*, **48**, No. 6, 1111–1125 (2008).
13. A. G. Kulikovskii, N. V. Pogorelov, and A. Yu. Semenov, *Mathematical Problems of Numerical Solution of Hyperbolic Systems of Equations* [in Russian], Fizmatlit, Moscow (2001).
14. V. S. Surov, Concerning a means of approximate solution of the Riemann problem for a single-velocity multicomponent mixture, *Inzh.-Fiz. Zh.*, **83**, No. 2, 351–356 (2010).